Climate Dynamics (2020) 54:3109–3120
https://doi.org/10.1007/s00382-020-05161-1

Mirror patterns of physical variables in the ocean

Gang Wang[1,2,3] · **Fangli Qiao**[1,2]

Received: 15 April 2019 / Accepted: 3 February 2020 / Published online: 13 February 2020

Abstract
Temperature and salinity are independent thermodynamic variables of seawater. However, it was determined from monthly Argo data that the correlation coefficient between layer-averaged temperature and salinity (T–S) time series peaks at a depth of approximately 300 m. Meanwhile, T–S patterns around that depth are consistent. Therefore, this layer is named "T–S mirror layer". Since the major feature of the T–S mirror layer is the high similarity of temperature and salinity patterns in it, spatial correlation should be a more direct way to determine it. Following this idea we introduce another kind of "T–S mirror layer", which resides at 100–200 m in four sets of objectively analyzed ocean data products (WOA13, EN4, Ishii and Argo). The "T–S mirror layer" derived in this way couples with the quasi-linear "slender waist" in T–S scatter diagrams; and this coupling is typical in mid- and low-latitude oceans. The slender waist in T–S scatter diagram implies that the profiles of temperature and salinity are in phase around it. We can then give a first guess for the depth of mirror patterns of two variables just according to their local profiles. Hereby, we find mirror patterns between other variable pair (e.g., temperature and sound velocity), inverse mirror patterns (i.e. the highest spatial correlation between variable pair, e.g., temperature and density, are negative), and malposed mirror patterns (spatial correlation peaks for variable patterns in different layers). This work reveals a phenomenon that bridges horizontal patterns of variable pairs in the ocean to their vertical profiles.

Keywords T–S mirror layer · Pycnocline · T–S scatter diagram · Inverse mirror patterns · Malposed mirror patterns

1 Introduction

In monthly Argo (Array for Real-time Geostrophic Oceanography) data, Chen and Geng (2019) found that the Pearson correlation between layer-averaged temperature and salinity (hereafter referred to as "T–S") time series peaks at approximately 300 m depth. Furthermore, the T–S patterns at that depth, both in climatology and seasonality, are consistent. They introduced the "T–S mirror layer" to term the particularly layer in which the patterns of temperature and salinity are similar. The "T–S mirror layer" is featured with six typical warm and salty pools in mid and low latitude. Therefore, Chen and Geng speculated that it was determined by dominant ocean circulations and mesoscale eddies in the pycnocline.

To evaluate the similarity of two spatial patterns, spatial correlation is a more direct way. This work will derive another kind of "T–S mirror layer" via spatial correlation between temperature and salinity patterns. The T–S mirror layer derived in this way possesses the same physical implications as that introduced by Chen and Geng (2019). However, the depths of these two kinds of mirror layers are not the same. For clarity, we use "T–S mirror layer" to refer in particular to that derived via the spatial correlation, while "α-T–S mirror layer" to that derived via Chen and Geng's approach. We will explain that the T–S mirror layer is closely related to a typical structure of T–S scatter diagram in mid- and low-latitude oceans: a "slender waist" in its mid part. By "slender waist" we mean that the T–S scatters in the central part of the diagram concentrate in a narrow quasi-linear band. A necessary condition for the existence of the T–S mirror layer will be given consequently. By virtue of

✉ Fangli Qiao
Qiaofl@fio.org.cn

[1] First Institute of Oceanography, Ministry of Natural Resources, Qingdao 266061, China

[2] Laboratory for Regional Oceanography and Numerical Modeling, Pilot National Laboratory for Marine Science and Technology, Qingdao 266237, China

[3] National Engineering Laboratory for Integrated Aero-Space-Ground-Ocean Big Data Application Technology, Qingdao 266061, China

this condition, we will derive some different kinds of mirror patterns of physical variable pair in the ocean.

2 Data and method

This work uses four objectively analyzed datasets, i.e. WOA13, EN4, Ishii, and Argo. All of them are openly available to the public.

WOA13 (World Ocean Atlas 2013) is a set of climatological mean, gridded fields of oceanographic variables (https://www.nodc.noaa.gov/OC5/WOA13/pr_woa13.html). It is based on direct in situ measurements from a wide variety of sources. And its variables include temperature, salinity, dissolved oxygen, and other parameters. Global, decadal averages of oceanographic variables are provided at monthly averaging periods and interpolated on 0.25° grids to 57 depths with a maximum depth of 1500 m. It also provides seasonal averaged variables interpolated on 0.25° grids to 102 depths with a maximum depth of 5500 m. In the Southern Ocean, deep sea or some other regions, data are constructed based on limited data. Computations therefore could render some meaningless.

EN4 (version 4 of the Met Office Hadley Centre "EN" series of datasets of global quality-controlled ocean T–S profiles and monthly objective analyses, https://www.metoffice.gov.uk/hadobs/en4/download.html) is a collection of ocean temperature and salinity profiles across the global oceans (Good et al. 2013). Data contained in it are sourced from the World Ocean Database (WOD) and the Coriolis dataset for ReAnalysis (CORA). Monthly temperature and salinity of ocean water are interpolated on 1° grids at 42 depths, with a maximum depth of 5,350 m. EN4 data span from 1900 to present. In this work, we use only those of the first 10 years in this century.

Ishii dataset provides global monthly subsurface temperature and salinity time varying maps (Ishii et al. 2005). The dataset starts in 1945 and covers the upper 1,500 m of ocean water at 24 standard layers on 1° grids. The analysis is based primarily on observed data from the World Ocean Atlas 2005 (WOA05). Some temperature and salinity in the tropical Pacific from IRD, and sea surface temperature from the Centennial in situ Observation Based Estimates (COBE) are also included. Ishii spans from 1945 till the end of 2012. Again we use only the 10-year monthly grid data in the beginning of this century.

Argo in this work is not the version used by Chen and Geng (2019). It is an analyzed 3D grid product produced by the China Argo Real-time Data Centre in 2013 (https://www.argo.org.cn). It covers latitudes from 60° S to 60° N, and spans from January 2004 to December 2011. Data of eight years are interpolated on 1° grids in 48 layers with a maximum depth of 1950 m.

Besides those analyzed datasets, the following discussion will also use global ocean model results of assimilation runs from FIOCOM (the First Institute Oceanography wave-tide-current Coupled Ocean Model) and SODA2.2.4 (version 2.2.4 of Simple Ocean Data Assimilation). FIOCOM is a 0.1°-grid global ocean circulation model coupled with wave mixing and tidal mixing. Two years' analyzed daily data (January 1, 2015 to December 31, 2016) are available at https://fiocom.fio.org.cn. Further details for this model please refer to Xiao et al. (2016). SODA (Carton et al. 2000) is a global circulation model product at 0.5° grids, whose time spans from 1871 to 2008. It can be found in https://iridl.ldeo.columbia.edu/SOURCES/.CARTON-GIESE/.SODA.

We will determine mirror patterns via the spatial correlation between maps of two variables. Spatial correlation between two 2D fields A and B is defined as

$$r = \frac{\sum_m \sum_n \left(A_{mn} - \overline{A}\right)\left(B_{mn} - \overline{B}\right)}{\sqrt{\sum_m \sum_n \left(A_{mn} - \overline{A}\right)^2}\sqrt{\sum_m \sum_n \left(B_{mn} - \overline{B}\right)^2}}, \quad (1)$$

where $\overline{A}$ and $\overline{B}$ are the respective spatial means of A and B.

Seawater library version 3.3 for Matlab (Phillip 2010) is used to calculate ocean water density, buoyancy frequency (Brunt-Väisälä frequency) and sound velocity in the ocean.

3 T–S mirror layer determined by spatial correlation

In upper ocean both temperature and salinity patterns represent a clear annual cycle. As a result, their spatial correlation varies seasonally. Figure 1a gives the spatial correlation coefficient between seasonal maps of temperature and salinity in WOA13, which is highest in winter and lowest in summer. In all the four seasons, the correlation profile increases with water depth until approximately 150 m, where it reaches a maximum (approximately 0.6). And the seasonal difference between the spatial correlations at that depth is less than 0.02. The depth at which the T–S spatial correlation peaking is the "T–S mirror layer". Downward till 200 m, the T–S spatial correlation keeps at a high value of about 0.6. It is commonly speculated that a stable temperature-salinity relationship might exist in most areas toward the deep layers (Gould and Turton 2006). At depths beyond the scope of Argo measurements (below 1975 m) T–S spatial correlation in WOA13 peaks again (as high as 0.75) at approximately 2400 m. However, ocean waters below 2000 m are quite homogeneous, i.e. both temperature and salinity fluctuate slightly in deep layers. The high spatial correlation at that depth actually provides little information. In addition, observations below

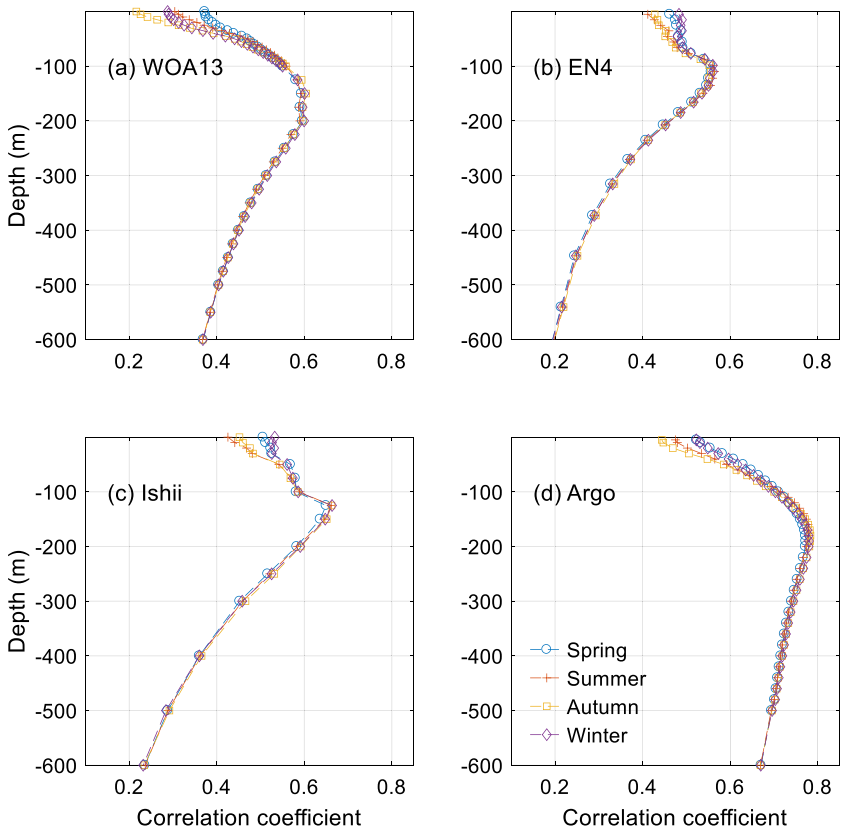

Fig. 1 Profiles of the spatial correlation coefficient derived from **a** WOA13, **b** EN4, **c** Ishii and **d** Argo

Table 1 Information in the T–S mirror layer in four datasets

Dataset	Resolution (°)	Depth of T–S mirror layer (m)	Spatial correlation between T&S patterns
WOA13	0.25	150	0.59
EN4	1	110	0.56
Ishii	1	125	0.66
Argo	1	180	0.78

2000 m are limited and thereby render greater uncertainty. Therefore, we focus on the extremum of the T–S spatial correlation in layers no deeper than 1000 m.

Figure 1b–d give the layered T–S spatial correlation in EN4, Ishii and Argo, respectively. Similar to what has been showed in Fig. 1a, seasonal variations of the T–S spatial correlation are great in the upper layers and decrease with depth. Each correlation profile reaches a maximum near the bottom of the mixed layer. The peak values and the depths of the T–S mirror layer in EN4, Ishii and Argo are listed in Table 1. Since EN4 covers the whole water column as seasonal WOA13 does, there are two additional maxima of T–S spatial correlation in EN4 at approximately 2400 m and 4800 m. As above, we do not view these two layers as candidates for a T–S mirror layer.

In any layer from ocean surface to bottom, the T–S spatial correlation in Argo is the greatest in the four datasets. One reason is that the Argo product covers only 60° S to 60° N, excluding samples from high-latitude areas. Those samples at high-latitude areas usually contribute negative to the T–S spatial correlation.

Figure 2 gives the temperature and salinity patterns in the T–S mirror layer in spring (similar to the results in the other seasons). In all the four datasets, the mirror patterns are featured with six warm and salty "tongues" extending eastward in the subtropics, as have likewise been noticed by Chen and Geng (2019) in the α-T–S mirror layer. The T–S mirror layers in EN4 and Ishii are shallower than that in the other two (WOA13 and Argo). And the temperature/salinity patterns in the T–S mirror layer are slightly different in the four datasets. Comparing the six warm and salty "tongues", WOA13 (Fig. 2a1, a2) and Argo (Fig. 2d1, d2) gives similar patterns, while EN4 patterns (Fig. 2b1, b2) are similar to Ishii's (Fig. 2c1, c2).

The fact that the T–S mirror layer was found in all the four analyzed datasets implies that the phenomenon is robust in the real ocean.

We notice that the T–S mirror layer seams much shallower than the α-T–S mirror layer. To confirm that these two kinds of mirror layers are not at the same depth, we calculate the Pearson correlation coefficient between the

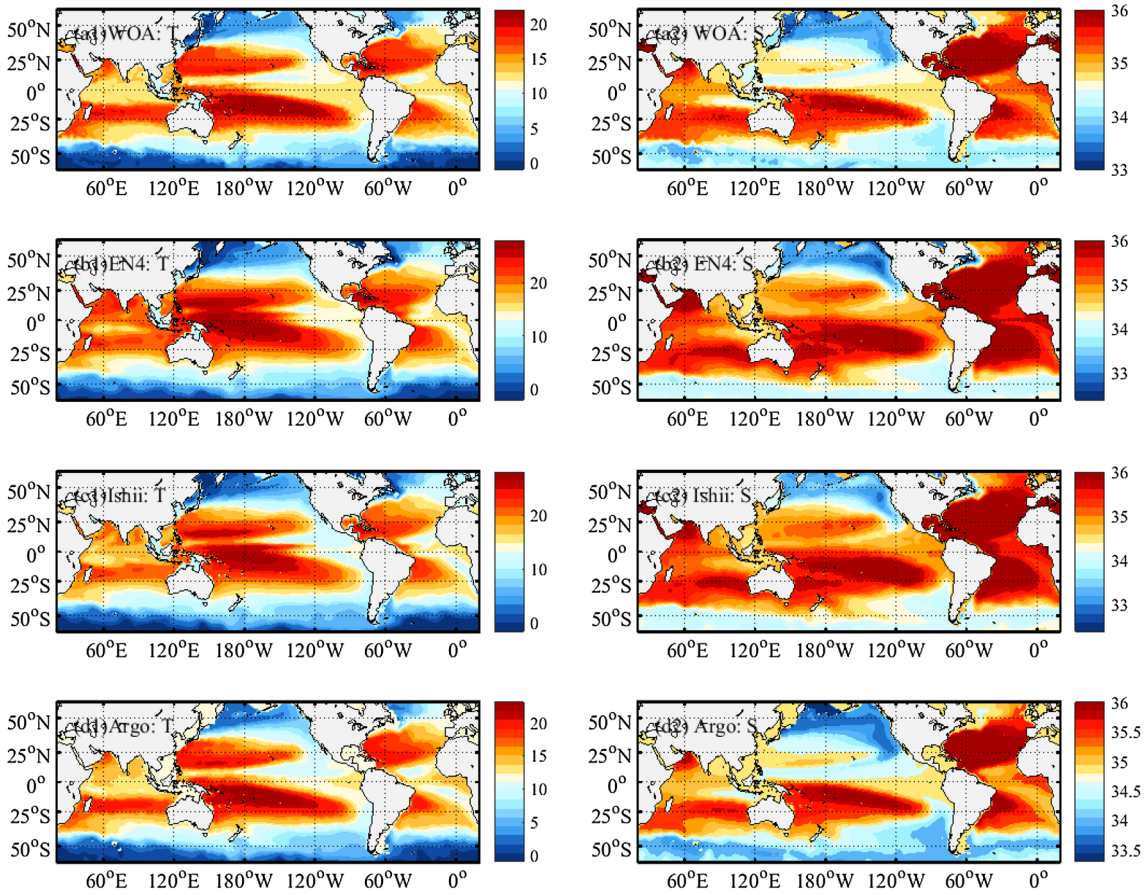

Fig. 2 Temperature (left column) and salinity (right column) patterns in the T–S mirror layer in **a1**, **a2** WOA13; **b1**, **b2** EN4; **c1**, **c2** Ishii; and **d1**, **d2** Argo

layer-averaged temperature and salinity time series in EN4, Ishii, and Argo. WOA13 are not used here since it provides only climatology fields. The correlation coefficient profile from EN4 is similar to that given by Chen and Geng, while the other two are quite different from it (Fig. 3).

The depth of the T–S mirror layer against the α-T–S mirror layer is given in Fig. 4a. In all the three datasets (EN4, Ishii and Argo), the T–S mirror layer is shallower than the α-T–S mirror layer. In fact, the deriving of the α-T–S mirror layer already implies that the Pearson correlation between T–S time series in the α-T–S mirror layer is greater than that in the T–S mirror layer. Their comparison is given in Fig. 4b. This outcome also reminds us that the T–S spatial correlation in the T–S mirror layer is always greater than that in the α-T–S mirror layer. The differences between these two kinds of mirror layers are summarized in Table 2.

There are at least two reasons why these two kinds of mirror layers are so different. First, α-T–S mirror layer has nothing to do with the temperature and salinity patterns, but the fluctuation of them. Therefore, those points with larger T/S fluctuations contribute greater weight in the averaged time series. The effects of those points on

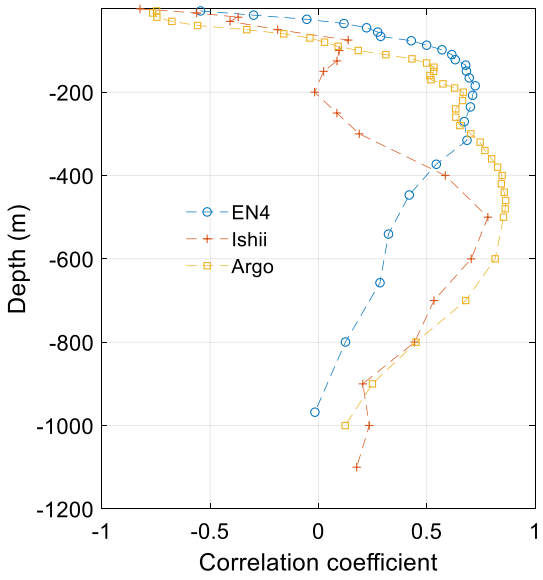

Fig. 3 Correlation coefficient profiles of layer-averaged T–S time series from EN4, Ishii and Argo

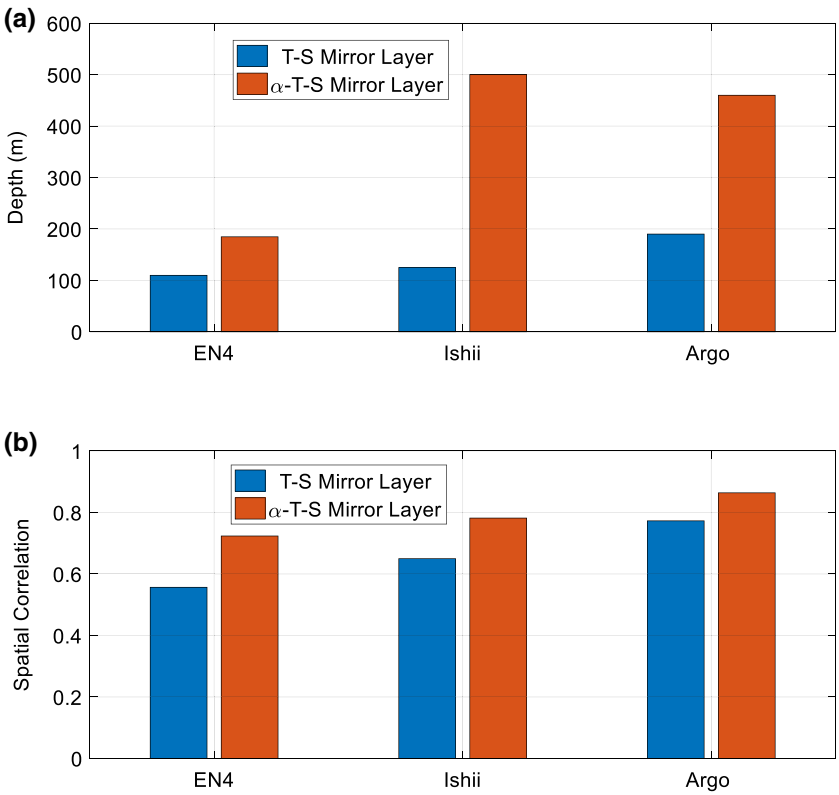

Fig. 4 **a** Depth of the T–S mirror layer and the α-T–S mirror layer derived from Ishii, WOA13 and Argo; and **b** correlation coefficient between layer-averaged temperature and salinity time series in the T–S mirror layer and the α-T–S mirror layer

Table 2 Comparison of the T–S mirror layer and the α-T–S mirror layer

	Depth	Correlation between layer average time series	Spatial correlation between two patterns
T–S mirror layer	Shallower	Smaller	Greater
α-T–S mirror layer	Deeper	Greater	Smaller

the variance of time series are amplified. Second, grids at higher latitude cover smaller areas in spherical coordinates. Their weights on the spatial averaged time series tend to be amplified if neglecting the effect of area size. For T–S mirror layer, points in high latitudes decrease the spatial correlation; while for α-T–S mirror layer, those points just decrease the fluctuation of averaged time series, which may favor a higher correlation.

Although the T–S mirror layer is not consistent with the α-T–S mirror layer, they actually possess the same physical intrinsic of the ocean: the layer in which temperature and salinity patterns are quite similar. In this sense, the T–S mirror layer is derived via a more direct way and therefore gives higher similarity in T–S patterns. Next, we will discuss the background factors that lead to the high similarity of the T–S patterns. We believe that the T–S mirror layer relates to a typical feature of T–S scatter diagram in mid and low latitude.

4 "Slender waist" in T–S scatter diagram

T–S scatter diagram is a traditional approach to analysis the ocean water mass (for example, He and Cai 2012; Cheng et al. 2014). In mid and low latitude, the ocean waters in the mixed layer are of warm and salty; while in deep layers they are cold and less salty. We limit the samples in a local $2^\circ \times 2^\circ$ region to plot the T–S scatter diagram. The T–S scatters in each intermediate layer in the thermocline make roughly a monotonous line; and these lines overlap successively to form a "slender waist", as the box in Fig. 5a designated. The slender waist centers at about 200 m depth. Its slope, $\Delta\theta/\Delta S$, is the ratio of the vertical gradient of temperature to salinity. On the slender waist, both temperature and salinity decrease when density increases. However, the decrease of temperature and salinity exert opposite effect on the change of density.

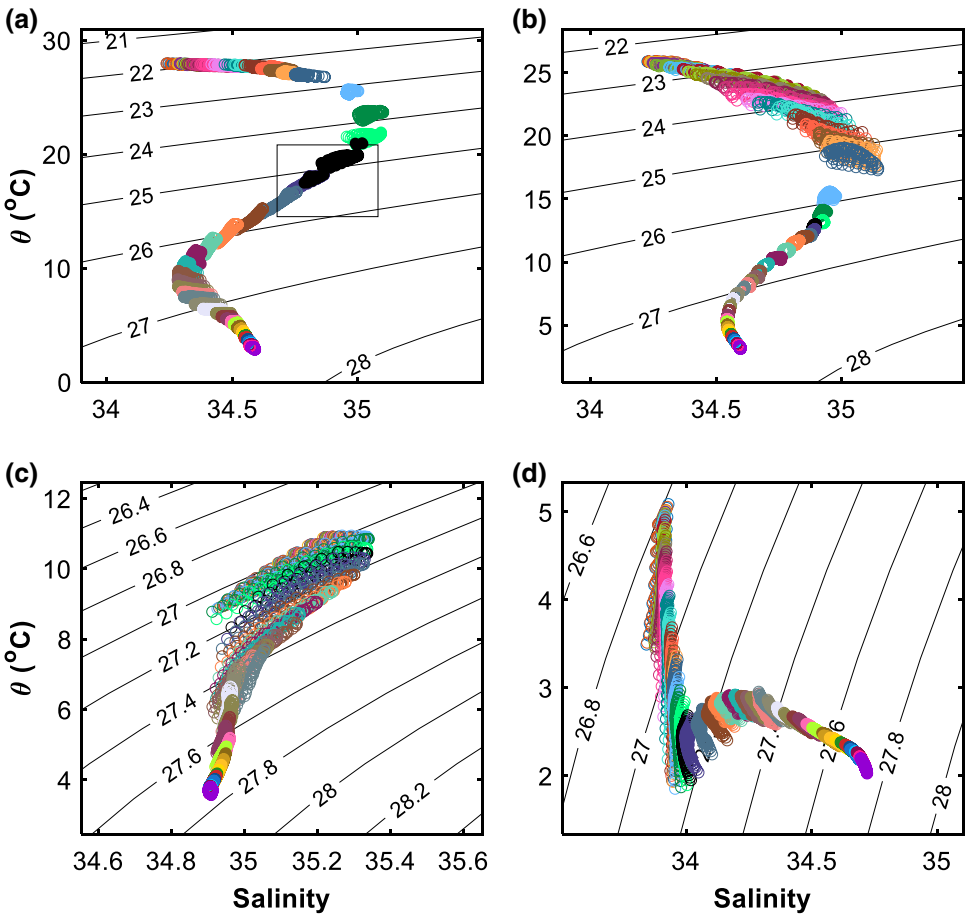

Fig. 5 T–S scatter diagrams in January, from WOA13 monthly climatology. Dots with the same color are samples in the same layer, and black dots are from 200 m depth. In **a** subtropical (140° E–142° E, 13° N–15° N) and **b** tropical (118° W–120° W, 0°–2° N) oceans, the T–S diagrams have slender waists, and the T–S in each layer are more stable than that in high latitudes of **c** north sub-polar (28° W–30° W, 50° N–52° N) and **d** south sub-polar (168° W–170° W, 58° S–60° S) areas

Specifically, the increase of density due to temperature is partly compensated by that due to salinity; however, the effect of temperature is dominant in the density variation. The T–S scatter diagram shows that the most stable layer locates at approximately 60 to 300 m depth, where the T–S scatters concentrate in a narrow band.

The "z"-shaped T–S scatter diagram is typical for tropical and subtropical oceans until latitude from approximately 45° S to 35 °S in the southern hemisphere, where the Deacon Cell transports 15 Sv (1 Sv = 10^6 m^3/s) water from the sea surface down to approximately 2,500 m without crossing any isopycnals (Döös 1994). In high-latitude oceans, T–S scatters in each layer are less concentrated, while water density varies in a narrow range (Fig. 5c, d). Therefore, T–S scatters in a layer found components either perpendicular to or parallel to the isopycnic. The waters corresponding to the parallel component are of different spicity (Huang 2011); i.e. they are either of high-temperature, high-salinity or of low-temperature, low-salinity. In each layer, the water density is rather stable. For the perpendicular component, both temperature and salinity increase when the density increasing. Salinity, rather than temperature, dominates the variation of the density. T–S patterns in high-latitude areas may reduce the spatial correlation in the global T–S mirror layer.

In Fig. 5d, the isopycnic is almost perpendicular to T–S scatters in each layer, suggesting that the horizontal gradient of density is much greater than the vertical. It indicates that the samples are near a front. For polar areas, 27.4-σ-isopycnic or 34-isohaline might be important in that the T–S scatters around it are almost linear. In contrast to that in low-latitude area (Fig. 5a, b), the temperature and salinity scatters in sub-polar regions are still in a quasi-linear line but of negative slope (Fig. 5d).

The slender waist, scatters around a quasi-linear line with positive slope, centers at approximately 15 °C (see Fig. 5a, b). Temperature on the waist ranges from 10 °C to 20 °C. Note that in tropical and subtropical oceans, the depth of 15 °C-isotherm is almost the T–S mirror layer. It then suggests that the T–S patterns around the 15 °C-isotherm are very similar. In fact, when the samples from a same layer concentrate around a line in T–S scatter diagram, it implies that temperature and salinity in that layer correlate linearly. That is, warmer water is also salter, and colder water fresher. Two patterns are mirroring in an area only when the horizontal gradients of the variables increase or decrease simultaneously. Note that the sample dots in T–S scatter diagram are from a local area (water column), but not from a profile. The slender waist in T–S scatter diagram guarantees that the

temperature pattern mirrors the salinity in the local area. In each small local area, the slender waist in T–S scatter diagram implies a pair of similar T–S patterns. Extending the local patterns continuously to larger areas yields the T–S mirror patterns. Eventually we find that the slender waist of T–S scatter diagram is in fact the other side of the T–S mirror layer.

Now we have explained that the slender waist in T–S scatter diagrams, which is typical in low-latitude oceans, is just a local manifestation of the T–S mirror layer in the subsurface ocean. Next, we will try to find an intuitive condition to locate the T–S mirror layer.

5 A necessary condition for T–S mirror patterns

The slender waist in T–S scatter diagram indicates that the temperature roughly linear correlates to salinity in several neighboring layers. That is, the temperature profile in these layers is in phase with the salinity profile. In mid and low latitude, ocean temperature under the mixed layer usually decreases with depth. Salinity however does not. In most vertical range of ocean water, salinity profile shows an increasing trend. An exception occurs in a shallow range around the pycnocline, where the water salinity decreases sharply with depth. In this range, the salinity profile is accordant with that of temperature. As an example, Fig. 6a shows a pair of temperature and salinity profiles at (119° W, 1° N), in which both temperature and salinity profiles decrease from 100 to 300 m. The similar feature is found at other low-latitude stations, such as (141° E, 16 °N) in Fig. 6b. In-phase feature of T–S profiles is a natural corollary of the slender waist in typical T–S scatter diagram.

The T–S mirror layer in this work also features with six warm and high salty pools in low-latitude area, as were found in the α-T–S mirror layer (Chen and Geng 2019). At the warm pool regions, the intrusion of high salinity waters makes the salinity profile increase with depth and then decrease in sub surface (Fig. 6a, b). It leads to a consistent change of temperature and salinity between 100 and 300 m. We have discussed that the consistent profiles could be deduced from the mirror patterns at the center of that range. The typical feature of temperature and salinity profiles in

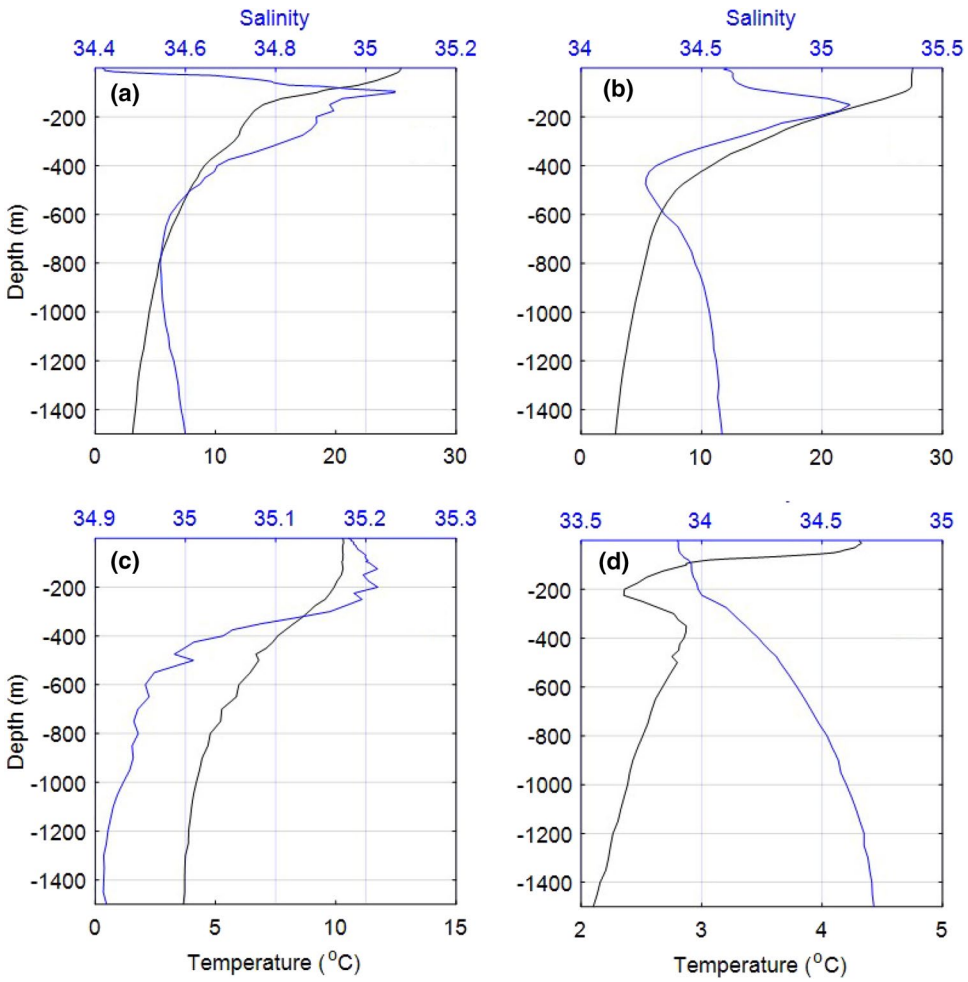

Fig. 6 Temperature and salinity profiles at four stations: **a** (119° W, 1° N), **b** (141° E, 16° N), **c** (29° W, 51° N), and **d** (169° W, 59° S). Data are from WOA13

the warm pools explains how the large-scale circulation and mid-scale eddies effects on the mirror layer.

In high-latitude areas (Fig. 6c, d), there are several peaks in either temperature or salinity profile. For instance, at (29° W, 51° N), salinity in the upper 300 m varies around 35.2. There are three maxima in this shallow water column (Fig. 6c). Therefore, it is difficult to find a range in which the trends of temperature and salinity profiles are consistent. Besides, both temperature and salinity in high latitude vary in their respective shallow range. The vertical temperature/salinity difference between neighboring layers is no greater than that between horizontal neighboring grids. At (169° W, 59° S), salinity profile is monotonous while temperature profile presents turning points at about 200 m (Fig. 6d). The only range that temperature and salinity being in phase is between 200 and 300 m. However, temperature and salinity patterns at these depths correlate negatively.

A variable's spatial pattern is depicted by its horizontal variances. Therefore, it is the local horizontal gradient rather than the relative difference of remote stations that determines a pattern. When temperature and salinity sampled in a local area tracing out a line in a T–S regime, they contribute consistently to the spatial correlation coefficient [Eq. (1)]. A high spatial correlation coefficient does not require that higher temperature should correspond to higher salinity in the whole area. As long as the variations of two variables coincide in each local area, the similarity of their patterns could be inferred by extending the local features to larger area.

T–S mirror patterns imply a slender waist in T–S scatter diagram, and slender waist then renders in-phase profiles of temperature and salinity in a range. Together, it means that the in-phasing feature of variable profiles is a necessary condition for mirror patterns. It provides a direct and simple clue to find the possible mirror patterns of two variables. That is, we can make a first guess on the possible range of mirror patterns according to variables' vertical profiles.

Now we describe the above discussion in mathematical formula. Suppose temperature and salinity patterns mirror each other. It means that for those T–S samples at each local area, higher temperature corresponds to higher salinity. Local area here refers to an ideal sample area in which temperature and salinity are one-to-one. That is, for each value of temperature, there is only one corresponding value of salinity and vice versa. Note that local area is a water column, but not a profile.

As illustrated in Fig. 7a, we denote the temperature and salinity in k-th layer and n-th grid by $T(x_n, z_k)$ and $S(x_n, z_k)$, respectively. Suppose that the deviation of both temperature and salinity in k-th layer is less than half of their respective vertical gradient, i.e.

$$\max_{i,j\in\Omega}\left|T_{i,k}-T_{j,k}\right| < 0.5\min_{i,j\in\Omega}\left|T_{i,k-1}-T_{j,k}\right|, \tag{2}$$

and

$$\max_{i,j\in\Omega}\left|T_{i,k}-T_{j,k}\right| < 0.5\min_{i,j\in\Omega}\left|T_{i,k}-T_{j,k+1}\right|. \tag{3}$$

Likewise for salinity.

These conditions implies that samples from three successive layers $k-1$, k and $k+1$ in local area Ω distribute in three boxes in a T–S diagram without overlapping (Fig. 7b). Any sample from these three layers gives monotonous temperature or salinity profile. Conditions (2) and (3) will be satisfied when the vertical gradients of temperature is great enough, likewise for salinity. In tropical and subtropical oceans, temperature decreases almost 10 °C from 200 m down to 300 m. Meanwhile, salinity decreases over 0.5 in the same range. The strong vertical gradient makes it possible to satisfy the above conditions. It is why the T–S mirror layer is found near the pycnocline. These condition guarantees that the temperature and salinity samples at (x_{n-1}, z_k), (x_n, z_k) and (x_{n+1}, z_k) will make a monotonous line in the T–S scatter diagram, i.e. temperature positively correlates to salinity.

If the samples in a layer compose a slender waist in T–S scatter diagram, the means of temperature and salinity are also in the waist. Therefore, if T–$\overline{T}$ changes its sign, so does S–$\overline{S}$. From Eq. (1), every pair of temperature and salinity contributes the same effect to the spatial correlation

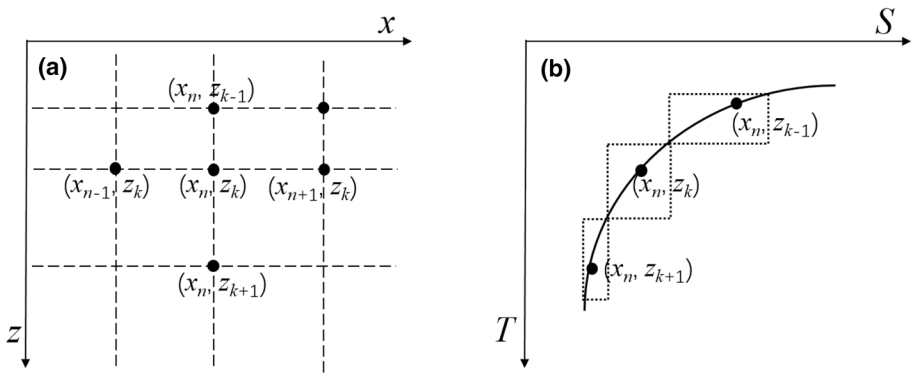

Fig. 7 **a** Sketch map of two-dimensional grids showing the sample area of temperature and salinity; **b** A T–S line sampled in three layers at a local area

coefficient. At the same time, when temperature and salinity profiles are in phase, the spatial correlation coefficient usually increases. If $T–\overline{T}$ changes its sign while $S–\overline{S}$ does not, it means that temperature and salinity are not one-to-one in the sample area. In this case, samples in three layers cannot be guaranteed in the three boxes without overlapping (Fig. 7b). Temperature and salinity profiles in this range then are not in phase. In this case, we do not expect to find mirror patterns in the local area.

On the other hand, monotonous profiles in a local area do not guarantee there being no overlap for samples in three boxes. So the in-phase feature of T–S profiles is only a necessary condition for the T–S mirror layer. Whatever, we can still use the profiles to give a first guess on the depth of mirror layer. The profiles are locally, so does the mirror patterns. A pair of global similar patterns should be reached by continuously extending the local feature to greater region.

6 Extensive mirror patterns

Besides temperature and salinity, there are still other physical variables in the ocean water: density, buoyancy frequency, sound velocity, etc. The necessary condition for the T–S mirror layer reminds us that there might be extensive mirror patterns of variable pairs at a depth where their profiles are monotonous and consistent. We use the WOA13 data in January to discuss these patterns.

6.1 Mirror patterns of other variables

The typical profile of sound velocity in ocean water is a three-layer structure. In the surface layer (mixed layer), gradient of sound velocity is negative, and varies seasonally. In the main pycnocline, the gradient is negative and varies slightly in season. In the deep oceans, the sound velocity is high and uniformly. The vertical profile of sound velocity in the ocean is similar to that of temperature. Therefore, mirror patterns of temperature and sound velocity are naturally expected. Figure 8 gives patterns of these two variables at 200 m. At that depth, the spatial correlation between temperature and sound velocity patterns (Figs. 6b and 8a) is over 0.99, much greater than that of temperature and salinity patterns (0.60). In fact, from 5 to 600 m depth, the spatial correlation between temperature and sound velocity patterns is always greater than 0.99. The spatial correlation between salinity and sound velocity patterns in that layer also reaches a high value of 0.61, slightly greater than that of temperature and salinity.

Buoyancy pattern also highly correlates to temperature (0.60) in 200-m layer. As Fig. 8c shows that the high-value tongues dominate the buoyancy pattern, just like the warm pools dominating the temperature patterns.

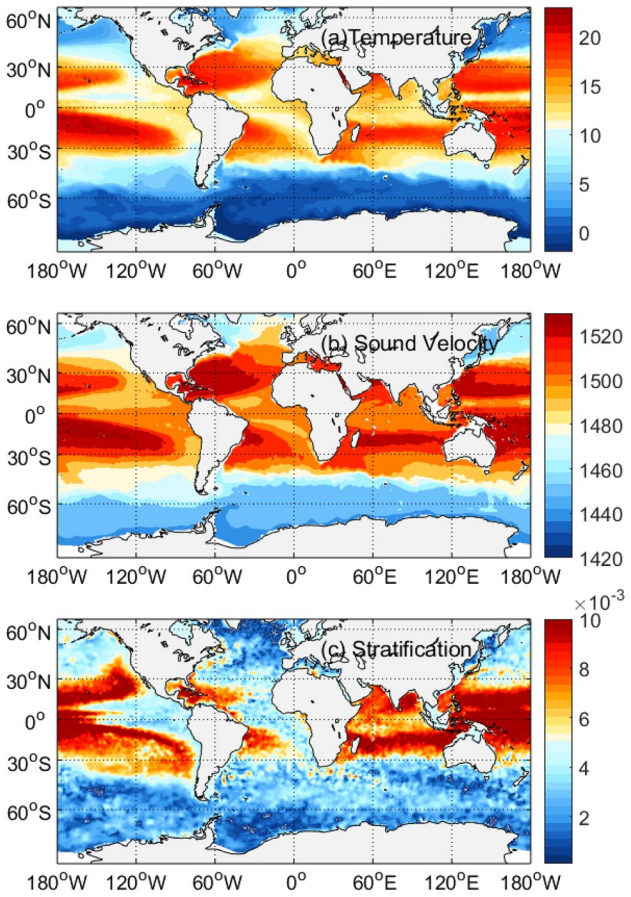

Fig. 8 **a** Temperature (unit: °C), **b** sound velocity (unit: m s^{-1}), and **c** stratification (Brunt-Väisälä frequency, unit: s^{-1}) patterns in the T–S mirror layer (200 m depth). The spatial correlation between temperature and sound velocity patterns is over 0.99, and that between temperature and Brunt-Väisälä frequency patterns is 0.60

6.2 Inverse mirror patterns

Figure 9 gives the temperature, salinity and density patterns in 200-m layer of WOA2013. The spatial correlation between temperature and salinity is 0.60, while that between temperature and density is − 0.80. Note that we use inverse color sequence for density contours in Fig. 9c. The highest (negative) spatial correlation (− 0.82) between temperature and density patterns however appears at 125 m, slightly shallower than the T–S mirror layer (150–200 m). Since temperature is the dominant factor to determine the density in the tropical upper ocean, it is not surprising to find inverse mirror patterns of temperature and density. In contrast, the spatial correlation coefficient between salinity and density patterns is nearly zero at around 200 m depth, and increases to 0.57 at approximately 600 m.

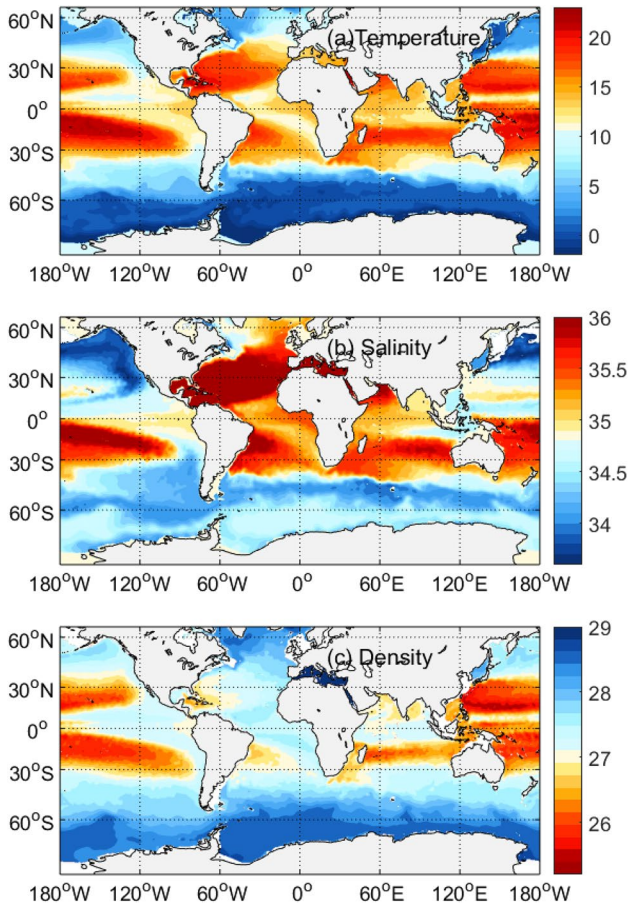

Fig. 9 **a** Temperature (unit: °C), **b** salinity, and **c** density (kg m^{-3}) patterns at 200 m depth in WOA2013. The spatial correlation between temperature and salinity patterns is 0.6, and that between temperature and density patterns is − 0.8. Note that the color sequence in density contour is reversed against the other two

6.3 Malposed mirror patterns

In the above discussion, we gave mirror patterns of physical variable pairs. In fact, the highest correlated patterns of two variables may come from different layers. Figure 10 gives the spatial correlation between temperature and one of the following variables: sound velocity, density, salinity and buoyancy frequency. The depth of the highest correlated patterns and the corresponding correlation coefficients are listed in Table 3.

The highest correlation between temperature and sound velocity is found at 500 m. Generally, temperature and sound velocity in the same layer has a high correlation coefficient greater than 0.99 (Fig. 10a). The highest (negative) correlation between temperature and density is also found when these two patterns are in the same layer (Fig. 10b).

In another way, the correlation between temperature and salinity peaks when temperature pattern is from 200 m while salinity pattern is from 325 m (Fig. 10c). The spatial correlation between malposed temperature and salinity patterns is greater than that in the T–S mirror layer.

For temperature and buoyancy frequency patterns, their spatial correlation peaks when they are from different layers. Say, temperature pattern from about 900 m while Brunt-Väisälä frequency pattern from about 500 m (Fig. 10d). In another word, temperature and Brunt-Väisälä frequency are of malposed mirror patterns.

7 Discussion

Large scale ocean circulations determine the temperature and salinity fields in the ocean. The coupling of T–S mirror layer and slender waist of T–S scatter diagram indicates that the T–S mirror layer is determined not only by the ocean circulation and mesoscale eddies, as has been suspected, but also by the thermodynamic processes in the ocean. In subtropical oceans, high evaporation and short wave irradiance throughout the year produce saltier and warmer waters in the surface layers; this outcome is typical in subtropical oceans. The slender waist in T–S scatter diagram bridges high-temperature, high-salinity seawater at the bottom of the mixed layer and low-temperature, low-salinity seawater in the deep ocean. Its quasi-linear waist yields that the T–S patterns mirror each other in a restricted vertical range. We proposed that the slender waist in the T–S scatter diagrams driven by short wave irradiance and evaporation-precipitation processes in the subtropical ocean surface waters.

In winter, strong mixing takes the high-temperature, high-salinity feature down to the bottom of the mixed layer. Stable circulation then drives the water in a stable horizontal pattern. By virtue of diffusive and internal mixing, vertical temperature/salinity gradients are formed between high-temperature, high-salinity waters at the bottom of mixed layer and low-temperature, low-salinity water in deep oceans. The effects of T–S variation on density compensate one another. Therefore, the density variation of seawater between mixed layer and deep oceans is small, although the actual density difference is rather great.

In summer, high precipitation and short wave irradiance produce fresher and warmer waters and thus a stronger stratification. However, the pycnocline is no deeper than the mixed layer depth in winter. Therefore, the T–S spatial correlation in upper ocean waters is lowest in summer and highest in winter (see Fig. 1). Nevertheless, seawater temperature and salinity between 100 and 300 m always decrease with depth. In deeper layers, small T–S gradients indicate that the variety of temperature or salinity is more localized and independent.

We should emphasize that only when T–S varies in a proper range we can locate the mirror layer. In high-latitude region such as the Antarctic, the T–S patterns in the T–S

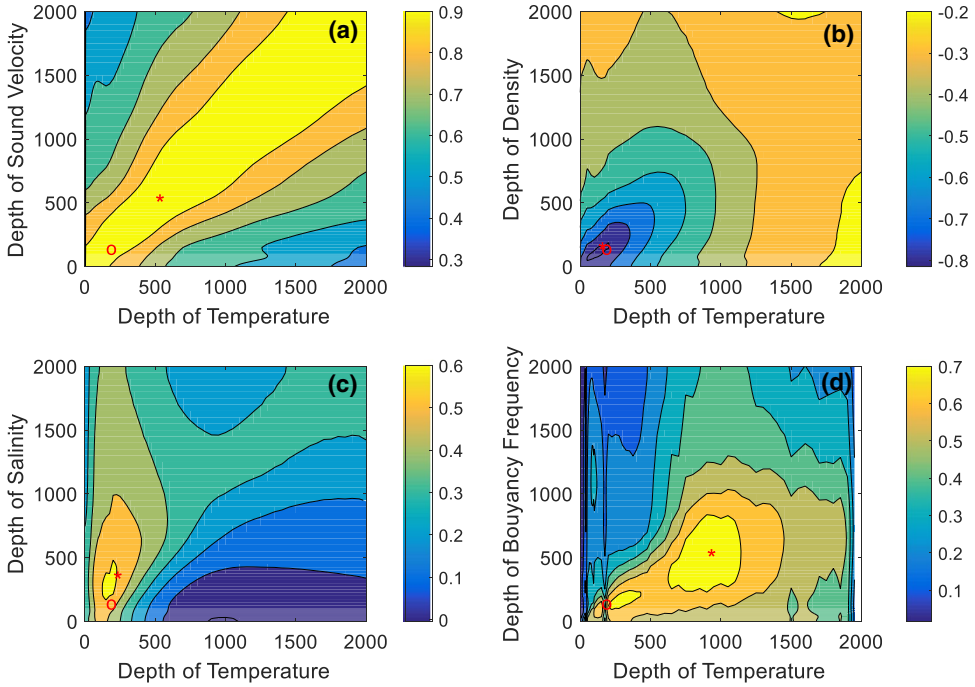

Fig. 10 Spatial correlation between temperature and one of the following variables: **a** salinity, **b** density, **c** sound velocity, and **d** Brunt-Väisäla frequency. Red circle in each panel is the position of T–S mirror layer (200 m in WOA2013), and red star is the position of mirror patterns between temperature and another variable from (**a**) to (**d**)

Table 3 The depths of malposed mirror patterns of two variables

	Depth (m/m)	Spatial correlation
Temperature/sound velocity	500/500	> 0.99
Temperature/density	125/125	− 0.82
Temperature/salinity	200/325	0.61
Temperature/buoyancy frequency	900/500	0.79

mirror layer are negatively correlated; i.e. warmer waters are fresher. In fact, the areas where temperature and salinity positively correlate in mirror patterns (Fig. 2) exist roughly in where the sea surface temperature is higher than 15 °C. It is not difficult to understand, since although the T–S scatters still vary quasi-linearly when $t > 20$ °C or $t < 10$ °C, their concentrated line presents a negative slope. It also explains why the T–S patterns in high latitude mirror inversely even in the T–S mirror layer.

The T–S mirror layer could also be found in numerical simulation results. Figure 11 gives snapshots of T–S patterns from the FIOCOM and SODA. The T–S mirror layer locates at 125 m in FIOCOM (April 30, 2015) and 171 m in SODA (April 30, 2008). The corresponding spatial correlation (0.55 in FIOCOM, 0.72 in SODA) is calculated for the global ocean while the patterns represented only from 60° S to 60° N. Compared with SODA, the spatial correlation between

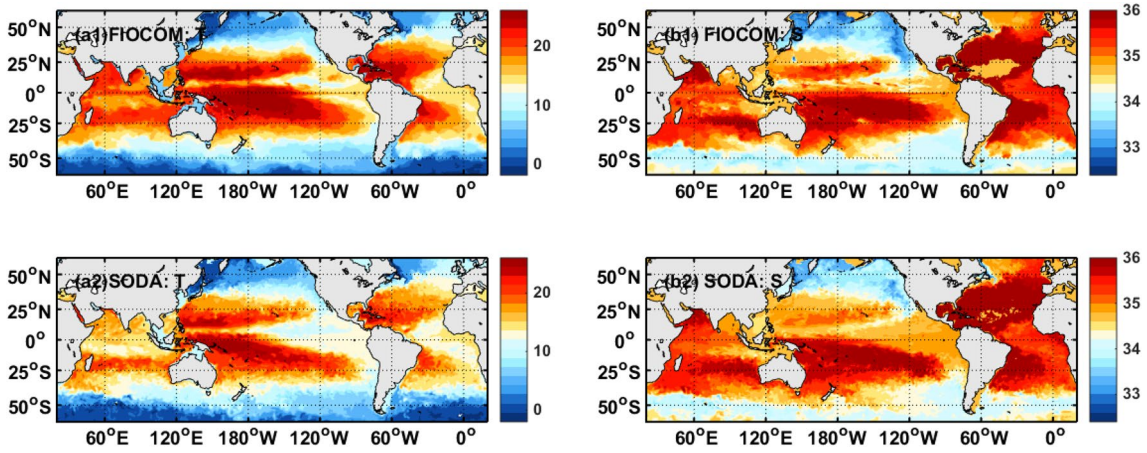

Fig. 11 Snapshots of **a1/a2** temperature and **b1/b2** salinity patterns at 125 m/171 m in FIOCOM/SODA (April 30, 2015/April 30, 2008). Spatial correlation coefficient between temperature and salinity patterns is 0.55/0.72

the temperature and salinity patterns in FIOCOM is smaller, and the corresponding mirror layer is shallower. However, the results from FIOCOM are closer to those derived from WOA13, EN4 and Ishii.

8 Conclusion

The T–S mirror layer and the quasi-linear slender waist in T–S scatter diagrams, which is typical in mid and low latitude oceans, are essentially "two sides of one coin". Each of them implies that temperature linearly correlates to salinity in a T–S range. In another word, the variations of temperature and salinity within the mirror layer are consistent.

The T–S mirror layer can be used to evaluate the performance of ocean general circulation models, both for thermal patterns and dynamic features. For example, we can compare the depth of the T–S mirror layer in two datasets, or the spatial correlation between temperature and salinity patterns in that layer. Another application of the T–S mirror layer is that once we obtained a pattern of either temperature or salinity in the mirror layer, we also got a general conception of the pattern for the other parameter.

This work also introduced extensive mirror patterns of physical variables in ocean data. Some are highly correlated at a particular depth; some correlate with a negative peak (negative mirror layer); and some are highly correlated for variables from different layers (malposed mirror patterns). The similarity of a pair of patterns tends to give a perception that there is a cause and effect relationship between the two variables. However, different mirror patterns presented in this work indicate that high spatial correlation between two variables may not suggest causality between them. For instance, the spatial correlation between temperature and salinity patterns is as high as 0.6 in the T–S mirror layer. As we know, they are actually almost independent of each other. The similarity of their patterns in a layer does not render that one of them determines the other. Another example is about the sound velocity. The spatial correlation between the sound velocity and either temperature or salinity is very high. Nevertheless, it does not imply that the sound velocity in the ocean is determinate by both temperature and salinity.

Acknowledgements G. Wang is supported by the National Key Research and Development Program of China Grant nos. 2016YFC1401407 and 2016YFB0201100, the National Natural Science Foundation of China under Grant no. 41476024, as well as the Natural Science Foundation of Shandong Province of China (ZR2017MD011); F. Qiao is supported by the NSFC-Shandong Joint Fund for Marine Science Research Centers of China Grant no. 41821004 and U1606405, the International Cooperation Project on the China-Australia Research Center for Maritime Engineering of Ministry of Science and Technology, China, Grant no. 2016YFE0101400 and the International Cooperation Project of Indo-Pacific Ocean Environment Variation and Air-Sea Interaction of contract no. GASI-IPOVAI-05.

References

Carton JA, Chepurin G, Cao X, Giese B (2000) A simple ocean data assimilation analysis of the global upper ocean 1950–95. Part I: Methodology. J Phys Oceanogr 30:294–310

Chen G, Geng D (2019) A "mirror layer" of temperature and salinity in the Ocean. Clim Dyn 52(1–2):1–13

Cheng G, Sun J, Zu T, Chen J, Wang D (2014) Analysis of water masses in the northern South China Sea in summer 2011. J Trop Oceanogr (in Chinese) 33(3):10–16. https://doi.org/10.3969/j.issn.1009-5470.2014.03.002

Döös K (1994) Semianalytical simulation of the meridional cells in the Southern Ocean. J Phys Oceanogr 24:1281–1293

Good SA, Martin MJ, Rayner NA (2013) EN4: quality controlled ocean temperature and salinity profiles and monthly objective analyses with uncertainty estimates. J Geophys Res Oceans 118:6704–6716. https://doi.org/10.1002/2013JC009067

Gould WJ, Turton J (2006) Argo-Sounding the oceans. Weather 61:17–21

He J, Cai S (2012) Study on the hydrological characteristic parameters and flow field east of the Luzon Strait using Argos profiling floats. J Trop Oceanogr (in Chinese) 31(1):18–27. https://doi.org/10.3969/j.issn.1009-5470.2012.01.003

Huang R (2011) Defining the spicity. J Mar Res 69(4):545–559

Ishii M, Shouji A, Sugimoto S, Matsumoto T (2005) Objective analyses of SST and marine meteorological variables for the 20th century using COADS and the Kobe Collection. Int J Climatol 25:865–879

Phillip PM (2010) Seawater library version 3.3 for Matlab. Maintained by Lindsay Pender, CSIRO

Xiao B, Qiao F, Shu Q (2016) The performance of a z-level ocean model in modeling the global tide. Acta Oceanol Sin 35(11):35–43